

# Effect of Adjacent Interval Width on Noise Properties of Striped Array Iron Core Fluxgate

Zhijun Cui\* and Xiaofei Jia

School of Electronic and Information Engineering, Ankang University, Ankang 725000, P. R. China

(Received April 11, 2022; accepted August 22, 2022)

**Keywords:** micro-fluxgate, array iron core film, noise properties, MEMS technology

In the field of weak magnetic field measurement, fluxgates have higher performance than other magnetic measurement devices. However, it is difficult to reduce fluxgate noise for miniaturized fluxgates. We present a new micro-fabricated iron core structure for a micro-fluxgate in this paper. The magnetization distribution near the edge of each iron core can be improved by adjusting the size and density of the striped array iron core. To investigate the magnetic characteristics of the striped array iron core and its effect on fluxgate noise, we increased the width of each iron core in the striped array core from 30 to 90  $\mu\text{m}$  in 10  $\mu\text{m}$  steps and the adjacent interval width of the striped array iron core from 25 to 45  $\mu\text{m}$  in 5  $\mu\text{m}$  steps. To measure the noise performance of the fluxgate, we used the striped array iron core to construct a flat structure fluxgate. The signal measurement showed that the noise of the fluxgate was related to the adjacent interval width of the striped array iron core, whereas the noise of the striped array iron core was lower than that of a permalloy film with the same total length, width, and thickness as the striped array iron core. The decrease in noise in the flat structure fluxgate was due to the transverse anisotropic field generated by the magnetostatic coupling effect between the striped array iron cores, which readily induced the coherent rotation of the magnetic domains in the magnetization process. The coherent rotation weakened the incoherent jump, the main source of Barkhausen noise, in the domain wall displacement.

## 1. Introduction

A fluxgate is used to measure weak magnetic fields via the nonlinear relationship between the magnetic induction intensity  $B$  and the magnetic field intensity  $H$  of the high-conductivity magnetic iron core under the saturation excitation of an alternating magnetic field.<sup>(1)</sup> The first micro-fluxgate was fabricated using micro-electromechanical technology by Seitz in 1990, which opened up a promising direction for fluxgate research.<sup>(2)</sup> However, the magnetic properties of the soft magnetic films prepared by micro-fabrication technology were weaker than those of the same composite magnetic bulk materials.<sup>(3)</sup> The decrease in iron core volume leads to a sharp decline in the performance of the micro-fluxgate,<sup>(4)</sup> particularly a significant

---

\*Corresponding author: e-mail: [cui\\_zj\\_163@163.com](mailto:cui_zj_163@163.com)  
<https://doi.org/10.18494/SAM3936>

increase in noise.<sup>(5)</sup> At present, the noise level of a micro-fluxgate is greater than that of a traditional fluxgate.

Butta and Sasada proposed that the main source of noise of a fluxgate was the iron core, not the measuring circuit or excitation current.<sup>(6)</sup> According to the magnetization curve between the magnetic induction intensity  $B$  and the magnetic field intensity  $H$  of the iron core, when  $H$  becomes large, irreversible domain wall movement occurs. At this time, the magnetic induction intensity  $B$  of the iron core abruptly jumps, giving the magnetization curve a ladder shape.<sup>(7)</sup> In the field of micromagnetism, this phenomenon is usually called the Barkhausen jump. This jump in magnetic induction intensity inside the iron core generates a signal similar to noise in the fluxgate detection coil, which is the Barkhausen noise of the fluxgate.<sup>(8)</sup> Moreover, the Barkhausen noise is the main noise in an iron core.<sup>(9)</sup> Decreasing the Barkhausen noise is the key element in reducing the noise of fluxgates.

It has been reported that low-noise soft magnetic materials have a relatively low Curie temperature, minimal magnetostriction, and minimal eddy current loss.<sup>(10,11)</sup>  $\text{Ni}_{81}\text{Fe}_{19}$  and cobalt-based amorphous materials, which are low-noise soft magnetic materials, are usually preferred for preparing the iron cores of fluxgates. Although changing the fabrication process and annealing the soft magnetic material used can reduce the noise of fluxgates, these methods are not effective in reducing the noise of micro-fluxgates.

Delevoye *et al.* prepared multilayer  $\text{Ni}_{82}\text{Fe}_{18}$  thin films as the iron core of a micro-fluxgate by sputtering.<sup>(12)</sup> Upon increasing the frequency of the fluxgate excitation signal to 100 MHz, the static magnetic coupling between the multilayer  $\text{Ni}_{82}\text{Fe}_{18}$  films restrained the closed magnetic domain in the direction of easy magnetization and reduced the noise of the micro-fluxgate. Although the noise of the fluxgate with an iron core length of only 1.56 mm was 5 nT/ $\sqrt{\text{Hz}}$  at 10 Hz, the noise at 1 Hz was still very large.

Fan *et al.* studied a multicore vertical fluxgate and found that its sensitivity increased exponentially with the number of iron cores. On the other hand, the noise level depended on the arrangement of iron cores and the working mode of the fluxgate, and was unrelated to the number of iron cores.<sup>(13)</sup> Ripka *et al.* also studied such a vertical excitation fluxgate of the same size and found that the noise of the fluxgate with four iron cores was reduced to 120 pT/ $\sqrt{\text{Hz}}$  at 1 Hz under an excitation signal of 20 mA current.<sup>(14)</sup> Although the volume of these two vertical fluxgates was small, the traditional method was still used to wind the measuring coil (1015 turns), which belongs to the traditional structure of the fluxgate. This noise reduction technology can be used as a reference for micro-fluxgates.

Skidanov showed that adjusting the size and density of narrow striped array iron cores could improve the magnetization distribution near the edge of the iron cores.<sup>(15)</sup> This method can adjust the magnetic properties of narrow striped array iron cores and improve the resolution of the fluxgate.

Multilayer  $\text{Ni}_{82}\text{Fe}_{18}$  thin films, the arrangement of the iron cores of the vertical excitation fluxgate, and narrow striped array cores are all used to reduce the noise of micro-fluxgates by changing the topology structure of the iron cores. In this paper, we study the effects of the width of each iron core in the narrow striped array cores and the adjacent interval width of the striped array iron cores on the noise of the micro-fluxgate while maintaining the total length, width, and thickness of the narrow striped array cores constant.

## 2. Fabrication of Striped Array Iron Core

The electroplating of the array iron cores in this study was based on a micro-electromechanical system (MEMS) process, which was composed of photolithography and electroplating processes. The process of fabricating the striped array iron core is shown in Fig. 1. Firstly, a 4-inch silicon wafer of 500  $\mu\text{m}$  thickness was used as the substrate, and a 300-nm-thick  $\text{SiO}_2$  layer was deposited on the surface of the silicon wafer by wet oxygen oxidation as an insulating layer. Subsequently, a Cu seed layer of 90 nm thickness was deposited on the  $\text{SiO}_2$  layer by magnetron sputtering. During the sputtering process, the substrate was kept at 200  $^\circ\text{C}$  to increase the adhesion between the Cu seed layer and the substrate. Then, a photoresist (EPG533) of 1.5  $\mu\text{m}$  thickness was spin-coated on the Cu seed layer, and the mold of the electroplated striped array iron core was fabricated by photolithography with the striped array iron core used as a mask.

Table 1 shows the electroplate liquids of different materials and the process parameters. During the electroplating process, the direct current density was set as 3  $\text{A}/\text{dm}^2$  for 3 min, the width of each iron core in the striped array iron core was varied from 30 to 90  $\mu\text{m}$  in 10  $\mu\text{m}$  steps, and the adjacent interval width of the striped array iron core was increased from 25 to 45  $\mu\text{m}$  in 5  $\mu\text{m}$  steps. The amount of striped array iron cores was 35 groups. The total thickness of the striped array cores was measured to be about 1.2  $\mu\text{m}$  using a DektakXT step analyzer. One of the striped array iron core samples fabricated by electroplating is shown in Fig. 2 (the width of each iron core in the striped array iron core is 40  $\mu\text{m}$  and the adjacent interval width of the striped array iron core is 35  $\mu\text{m}$ ).

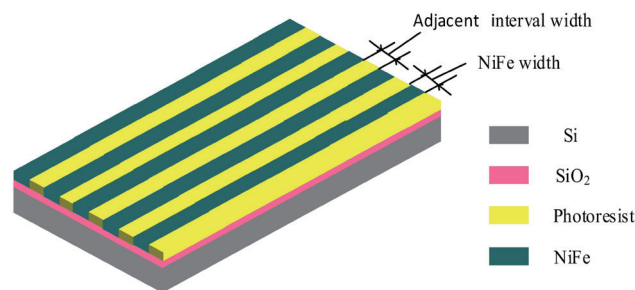


Fig. 1. (Color online) Process of fabricating striped array iron core.

Table 1  
NiFe electroplate liquids and process parameters.

Electroplate liquid (process parameters)	Liquid concentration
Nickel sulfate ( $\text{NiSO}_4 \cdot 6\text{H}_2\text{O}$ )	150 g/L
Nickel chloride ( $\text{NiCl}_2 \cdot 6\text{H}_2\text{O}$ )	75 g/L
Ferrous sulfate ( $\text{FeSO}_4 \cdot 7\text{H}_2\text{O}$ )	15 g/L
Boric acid ( $\text{H}_3\text{BO}_3$ )	45 g/L
Sodium tartrate (stabilizer)	15 g/L
Saccharin (softener)	2.5 g/L
Lauryl sodium sulfate (wetting agent)	0.3 g/L
KS-3000 (brightener)	0.6 mL/L
Temperature	57 $^\circ\text{C}$
pH	3

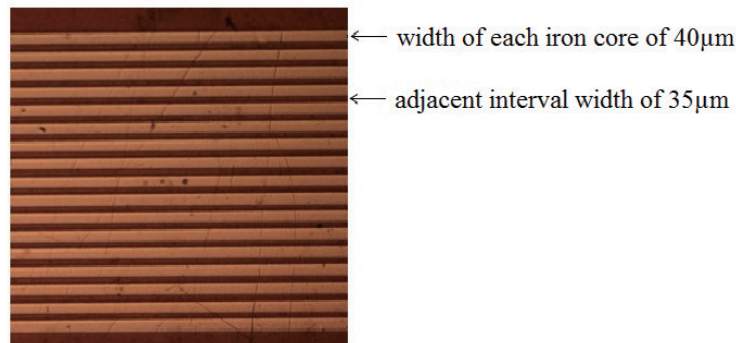


Fig. 2. (Color online) SEM image of fabricated striped array iron core with width of each iron core of  $40\ \mu\text{m}$  and adjacent interval width of  $35\ \mu\text{m}$ .

### 3. Noise Measurement of Striped Array Iron Cores

#### 3.1 Noise measurement system

We created a measurement system to measure the noise of the flat structure fluxgate composed of striped array iron cores prepared by electroplating. The principle of the measurement system is shown in Fig. 3. The excitation signal of the fluxgate was generated by cascading a signal generator (Agilent 33220A) and a power amplifier (NFHSA4011). An amperometer (Agilent 34401A) was placed in series with the excitation circuit to measure the excitation current.

A DC power supply (Agilent E3610A) drove the solenoid to generate an external magnetic field, while the excitation current was measured using the amperometer. An oscilloscope (Agilent Oscilloscope Infiniium 54830D) or a spectrum analyzer (Tektronix RSA 5103A) was connected to detection coils to measure and analyze the output voltage signal of the fluxgate.

A magnetic shielding device was used to exclude the effect of the geomagnetic field in the measurement of the fluxgate to simulate the zero-magnetic-field space in actual measurement.

#### 3.2 Noise measurement of striped array iron cores

To measure the noise performance of each striped array iron core sample as well as a permalloy film with the same total length, width, and thickness as the striped array core, a dual iron core fluxgate was constructed as shown in Fig. 4. Excitation and detection coils were wound around two “skeletons” with the same size and structure using the copper wire with a diameter of  $0.1\ \text{mm}$ . The excitation coils were wound clockwise for a total of 315 turns and the resistivity was  $7\ \Omega$ . The detection coils were wound counterclockwise for a total of 1150 turns and the resistivity was  $32\ \Omega$ . These two skeletons were hollow structures in which the striped array iron cores were placed.

The frequency of the sinusoidal excitation current was set to  $10\ \text{kHz}$  and the external magnetic field was set to  $30\ \mu\text{T}$ . The output signal of the fluxgate was processed using a

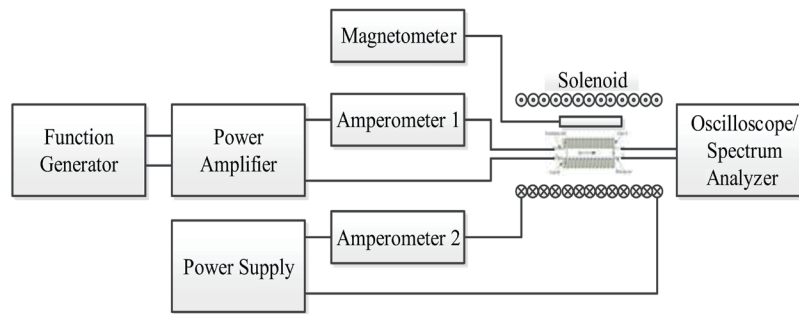


Fig. 3. Principle of system for measuring noise properties of micro-fluxgate.

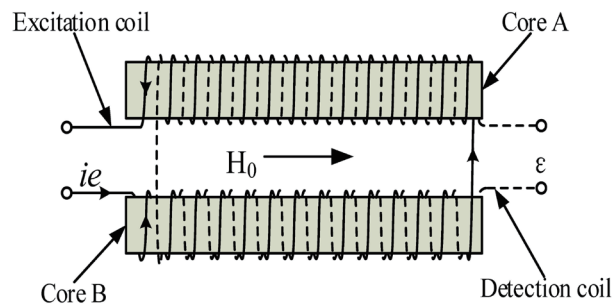


Fig. 4. (Color online) Dual iron core fluxgate.

spectrum analyzer (Tektronix RSA 5103A) to obtain the noise data in dBm units, which was then converted into the power spectral density of the magnetic noise.

On the basis of the principle of fluxgate noise measurement shown in Fig. 3, the noise properties of the 35 striped array iron cores and the permalloy film were measured and are shown in Fig. 5.

#### 4. Results and Discussion

From the experimentally obtained noise properties in Fig. 5, it can be seen that the noise of the striped array iron cores was greater than that of the permalloy film at 1 Hz for the adjacent interval widths of 25, 30, and 45  $\mu\text{m}$ . In contrast, when the adjacent interval width was 35 or 40  $\mu\text{m}$ , the noise of the striped array iron cores was half that of the permalloy film at 1 Hz. Therefore, the noise at 1 Hz was clearly dependent on the adjacent interval width of the striped array iron cores, i.e., the noise at 1 Hz can be reduced by selecting the suitable adjacent width of the striped array iron cores.

The relationship between the noise at 1 Hz and the adjacent interval width of the striped array iron core originated from the magnetostatic coupling effect between the striped array iron cores. When the adjacent interval width was increased from 25 to 45  $\mu\text{m}$  in 5  $\mu\text{m}$  steps, the change in the level of the magnetostatic coupling effect was first small, then large, and then small. These

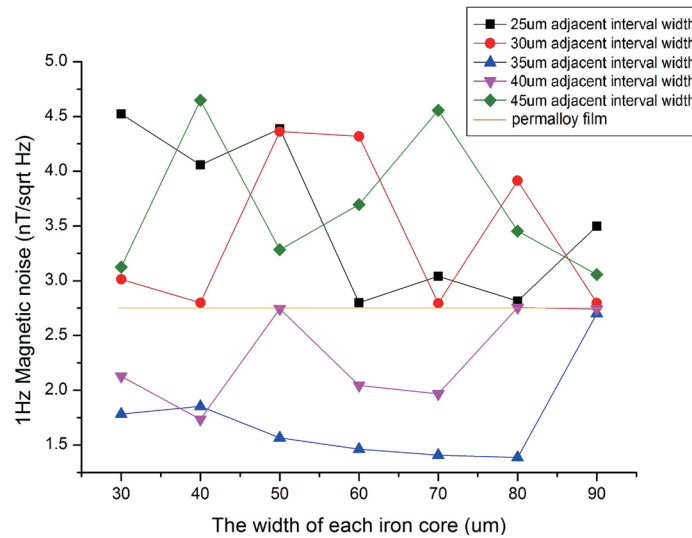


Fig. 5. (Color online) Noise properties of striped array iron cores and permalloy film at 1 Hz.

changes caused the angle between the internal magnetic moment and long-axis direction of the striped array iron cores to increase to  $90^\circ$  and then decrease. Then, the effects of the transverse anisotropic field (perpendicular to the long-axis direction of the striped array iron core) caused by the magnetostatic coupling effect tended to first be weak and then become strong as the adjacent interval width of the striped array iron core increased from 25 to 45  $\mu\text{m}$  in 5  $\mu\text{m}$  steps. The transverse anisotropic field generated by the magnetostatic coupling effect was similar to those generated by stress annealing,<sup>(16)</sup> stress electroplating,<sup>(17)</sup> magnetic field annealing,<sup>(18)</sup> and magnetic field electroplating.<sup>(19)</sup> During repeated magnetization, the magnetic domain readily rotated coherently, thus avoiding the incoherent jump in the displacement of the domain wall; this incoherent jump was the main reason for the Barkhausen noise at 1 Hz in the fluxgate.

To more clearly show the relationship between the fluxgate noise at 1 Hz and the adjacent interval width of the striped array iron core, we took the average fluxgate noise at 1 Hz for the adjacent interval widths of the striped array iron core of 25, 30, 35, 40, and 45  $\mu\text{m}$ . Figure 6 shows the average noise distribution at 1 Hz for these five values. From Fig. 6, it can be seen that the average fluxgate noise for an adjacent interval width of 35 or 40  $\mu\text{m}$  was smaller than that for 25, 30, or 45  $\mu\text{m}$  at 1 Hz.

On the basis of the principle of the reduced sum of the square minimum, the average fluxgate noise at 1 Hz was approximated using the function

$$y = a + \frac{c}{d + (x - b)^2}, \quad (1)$$

where  $x$  is the adjacent interval width of the striped array iron core,  $y$  is the average noise, and  $a$ ,  $b$ ,  $c$ , and  $d$  are coefficients.  $a$  was determined from the average noise of the fluxgate at 1 Hz, and  $b$ ,  $c$ , and  $d$  were determined from the adjacent interval width of the striped array iron cores. According to Fig. 6, Eq. (1) can approximately describe the variation in average noise at 1 Hz with the adjacent interval width of the striped array iron core.

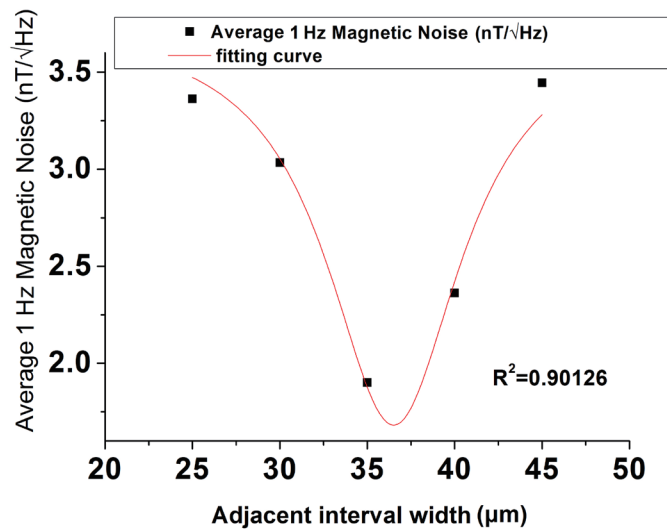


Fig. 6. (Color online) Average noise distribution at 1 Hz for different adjacent interval widths.

For  $x$  equal to 0 or  $\infty$ , the striped array iron core was regarded as a special case of the permalloy film. The noise at 1 Hz was smallest for a specific value of  $x$ . As a result, when fabricating a striped array iron core to decrease the noise of a micro-fluxgate, Eq. (1) can be used as a reference for selecting the optimal adjacent interval width of the striped array iron core.

## 5. Conclusions

In this paper, we reported the relationship between the adjacent interval width of the striped array iron core and the noise of a micro-fluxgate at 1 Hz. From the experiments, it can be seen that the transverse anisotropic field generated by the magnetostatic coupling effect prevented the incoherent jump of the domain wall, which was the main reason for the Barkhausen noise. The noise of the striped array iron core at 1 Hz was clearly dependent on the adjacent interval width of the striped array iron core. The noise at 1 Hz could be minimized by selecting the appropriate adjacent interval width of the striped array iron core.

## Acknowledgments

This work was partly supported by the Fundamental Research Funds for the National Natural Science Foundation of China (Grant No. 61801005) and the Natural Science Foundation of Shaanxi Province (Grant No. 2022JM-391).

## References

- 1 P. Ripka and S. W. Billingsley: IEEE Trans. Magn. **34** (1998) 1303. <https://doi.org/10.1109/20.706529>
- 2 T. Seitz: Sens. Actuators, A **22** (1990) 779. [https://doi.org/10.1016/0924-4247\(89\)80081-0](https://doi.org/10.1016/0924-4247(89)80081-0)
- 3 F. E. Rasmussen, J. T. Ravnkilde, P. T. Tang, O. Hansen, and S. Bouwstra: Sens. Actuators, A **92** (2001) 242. [https://doi.org/10.1016/S0924-4247\(01\)00556-8](https://doi.org/10.1016/S0924-4247(01)00556-8)

- 4 P. Ripka, S. Kawahito, S. O. Choi, A. Tipek, and M. Ishida: *Sens. Actuators, A* **91** (2001) 65. [https://doi.org/10.1016/S0924-4247\(01\)00481-2](https://doi.org/10.1016/S0924-4247(01)00481-2)
- 5 P. Ripka: *Sens. Actuators, A* **106** (2003) 8. [https://doi.org/10.1016/S0924-4247\(03\)00094-3](https://doi.org/10.1016/S0924-4247(03)00094-3)
- 6 M. Butta and I. Sasada: *IEEE Trans. Magn.* **48** (2012) 1508. <https://doi.org/10.1109/TMAG.2011.2173177>
- 7 P. Cizeau, S. Zapperi, G. Durin, and H. E. Stanley: *Phys. Rev. Lett.* **79** (1997) 4669. <https://doi.org/10.1103/PhysRevLett.79.4669>
- 8 J. Velázquez, C. García, M. Vázquez, and A. Hernando: *Phys. Rev. B* **54** (1996) 9903. <https://doi.org/10.1103/PhysRevB.54.9903>
- 9 H. Bittel: *IEEE Trans. Magn.* **5** (1969) 359. <https://doi.org/10.1109/TMAG.1969.1066547>
- 10 M. Butta, M. Janosek, P. Ripka, L. Kraus, and R. E. Kammouni: *IEEE Trans. Magn.* **50** (2014) 4006504-1. <https://doi.org/10.1109/TMAG.2014.2327105>
- 11 R. Bazinet, A. Jacas, G. A. B. Confalonieri, and M. Vazquez: *IEEE Trans. Magn.* **50** (2014) 6500103-1. <https://doi.org/10.1109/TMAG.2013.2292834>
- 12 E. Delevoye, M. Audoin, M. Beranger, R. Cuchet, R. Hida, and T. Jager: *Sens. Actuators, A* **145–146** (2008) 271. <https://doi.org/10.1016/j.sna.2008.01.018>
- 13 J. Fan, N. Ning, J. Wu, H. Chiriac, and X. P. Li: *IEEE Trans. Magn.* **45** (2009) 4451. <https://doi.org/10.1109/TMAG.2009.2023855>
- 14 P. Ripka, M. Butta, J. Fan, and X. P. Li: *IEEE Trans. Magn.* **46** (2010) 654. <https://doi.org/10.1109/TMAG.2009.2033554>
- 15 V. Skidanov: *J. Magn. Magn. Mater.* **320** (2008) e296. <https://doi.org/10.1016/j.jmmm.2008.02.061>
- 16 M. Tejedor, B. Hernando, and M. L. Sánchez: *J. Magn. Magn. Mater.* **140–144** (1995) 349. [https://doi.org/10.1016/0304-8853\(94\)00893-0](https://doi.org/10.1016/0304-8853(94)00893-0)
- 17 M. Butta, P. Ripka, and L. Kraus: *IEEE Trans. Magn.* **51** (2015) 4001104. <https://doi.org/10.1109/TMAG.2014.2358793>
- 18 P. Butvin, M. Janošek, P. Ripka, B. Butvinová, P. Š. Sr, M. Kuzminski, P. Š. Jr, D. Janičkovič, and G. Vlasák: *Sens. Actuators, A* **184** (2012) 72. <https://doi.org/10.1016/j.sna.2012.07.001>
- 19 M. Butta, P. Ripka, M. Janosek, and M. Pribil: *J. Appl. Phys.* **117** (2015) 17A722-1. <https://doi.org/10.1063/1.4914874>